Nucl Eng Technol 47 (2015) 139–147

Available online at www.sciencedirect.com

ScienceDirect

journal homepage: http://www.journals.elsevier.com/nuclear-engineering-and-technology/

Original Article

PREDICTION OF HYDROGEN CONCENTRATION IN CONTAINMENT DURING SEVERE ACCIDENTS USING FUZZY NEURAL NETWORK

DONG YEONG KIM, JU HYUN KIM, KWAE HWAN YOO, and MAN GYUN NA *

Department of Nuclear Engineering, Chosun University, 309 Pilmun-daero, Dong-gu, Gwangju 501-759, Republic of Korea

A R T I C L E I N F O

Article history:
Received 8 October 2014
Received in revised form
4 December 2014
Accepted 5 December 2014
Available online 21 January 2015

Keywords:
Fuzzy Inference System
Fuzzy Neural Network
Genetic Algorithm
Hydrogen Concentration
Loss of Coolant Accident
Severe Accident

A B S T R A C T

Recently, severe accidents in nuclear power plants (NPPs) have become a global concern. The aim of this paper is to predict the hydrogen buildup within containment resulting from severe accidents. The prediction was based on NPPs of an optimized power reactor 1,000. The increase in the hydrogen concentration in severe accidents is one of the major factors that threaten the integrity of the containment. A method using a fuzzy neural network (FNN) was applied to predict the hydrogen concentration in the containment. The FNN model was developed and verified based on simulation data acquired by simulating MAAP4 code for optimized power reactor 1,000. The FNN model is expected to assist operators to prevent a hydrogen explosion in severe accident situations and manage the accident properly because they are able to predict the changes in the trend of hydrogen concentration at the beginning of real accidents by using the developed FNN model.

1. Introduction

Recently, severe accidents in nuclear power plants (NPPs) have become a global concern. In the event of severe accidents, the major safety parameters of nuclear reactors change rapidly during the initial stages, leaving operators with insufficient time to devise an appropriate response. The efficient management of a serious accident requires observation of the key parameters during the very brief duration of initial events by establishing scenarios and initial events leading up to the accident. In particular, it is extremely important to determine safety-related parameters and critical information during the extremely short period following a loss of coolant accident (LOCA) and steam generator tube rupture (SGTR). This would enable verification of NPP status and determination of appropriate corrective action.

In case of severe accidents, the NPP operators are concerned about hydrogen explosion due to hydrogen accumulation in containment. Hydrogen is accumulated in containment by leakage from the primary pressure boundary.

* *Corresponding author.*
E-mail address: magyna@chosun.ac.kr (M.G. Na).

http://dx.doi.org/10.1016/j.net.2014.12.004

Special Issue on ISOFIC/ISSNP2014.

Therefore, this work considered severe incidents that were caused by LOCAs, which were analyzed by using data from optimized power reactor 1,000 (OPR1000). The work aimed to predict the hydrogen concentration in the event of a severe accident. The increase in the hydrogen concentration is one of the factors threatening the integrity of the containment. The hydrogen inside the containment is generated by the radio-activation of water in the atmosphere, corrosion of the inner material of the containment by containment spray, and reaction of steam with the zirconium cladding. Maintaining the integrity of the containment by preventing the hydrogen within from exploding would require the local hydrogen concentration to be retained below 4%.

Therefore, in this study, various artificial intelligence (AI) methods were examined to predict changes in the hydrogen concentration. It was determined that a method using a fuzzy neural network (FNN) was the most suitable for predicting the hydrogen concentration. A number of AI techniques have been applied successfully to a variety of research fields of nuclear engineering, such as signal validation [1–3], plant diagnostics [4–7], event identification [8–10], and smart sensing (or function approximation) [11–13]. Many of the previous works used fuzzy inference systems (FISs) and neural networks (NNs). Jang and Sun [14] demonstrated the functional equivalence between NNs and FISs in cases when the activation functions of the NNs and the membership function of the FIS are the same.

An FNN is a data-based model that requires data for its development and verification. As data from real severe accidents do not exist, it is necessary to use numerical simulations to obtain the required data for the proposed model. The FNN model was verified based on the NPP simulation data acquired using MAAP4 code [15]. The successful management of NPPs as a result of the ability to rapidly predict safety-critical parameters during real accidents could lead to the safekeeping of NPPs.

2. Fuzzy neural network

Fuzzy theory has been studied in an attempt to use a mathematical approach to prove the inaccuracy in human thoughts and actions. The FIS has been produced based on the concepts of intelligent *learning* and *inference*. An FNN model consists of an FIS combined with its neuronal training system.

2.1. Fuzzy inference system

FIS generally uses conditional rules that comprise the *if/then* rules of the antecedent part and consequent part, and it is one of the methods of AI [3]. Both the antecedent and consequent parts have membership functions capable of fuzzifying crisp values. In most cases, the Gaussian, triangular, trapezoid, and bell-shaped functions are used in the membership function formula.

Fig. 1 shows a pictorial sketch of the FIS principle [16]. The FIS output should be a real value that requires defuzzifying prior to forming the FIS output. Using a Takagi-Sugeno-type FIS that does not require the defuzzifier, an arbitrary i-th rule can be expressed as follows [17]:

$$\begin{aligned}&\textit{If } x_1(k) \text{ is } A_{i1}(k) \textit{ AND} \cdots \textit{AND } x_m(k) \text{ is } A_{im}(k), \text{ then}\\ &\widehat{y}_i(k) \text{ is } f_i[x_1(k), \cdots, x_m(k)]\end{aligned} \tag{1}$$

where $x_j(k)$ is the input variable to the fuzzy inference model ($j = 1, 2, \ldots, m$; m is the number of input variables), $A_{ij}(k)$ is the membership function of the j^{th} input variable for the i^{th} fuzzy rule ($i = 1, 2, \ldots, n$; n is the number of rules), and $\widehat{y}_i(k)$ is the output of the i^{th} fuzzy rule. In Equation 1, the function $f_i[x_1(k), \cdots, x_m(k)]$ represents a function of input variables. The membership functions of the fuzzy sets $A_{i1}, \cdots, A_{im}$ for the i^{th} fuzzy rule are denoted as $\alpha_{i1}(x_1), \cdots, \alpha_{im}(x_m)$, respectively.

The number of N input and output training data of the fuzzy model $\mathbf{z}^T(k) = [\mathbf{x}^T(k), y(k)]$ (where $\mathbf{x}^T(k) = [x_1(k), x_2(k), \cdots, x_m(k)]$ and $k = 1, 2, \cdots, N\alpha_{i1}$) were assumed to be available and the data point in each dimension was normalized. A Gaussian membership function was used because of the ability of this function to reduce the number of parameters to be optimized. Using a Takagi–Sugeno-type FIS, the output of the FIS can be expressed as follows [17]:

$$\widehat{y}(k) = \sum_{i=1}^{n} y_{wi}(k) \tag{2}$$

where

$$y_{wi}(k) = \overline{w}_i(k) f_i[\mathbf{x}(k)] \tag{3}$$

$$\overline{w}_i(k) = \frac{w_i(x(k))}{\sum_{i=1}^{n} w_i(x(k))} \tag{4}$$

$$w_i(k) = \prod_{j=1}^{m} \alpha_{ij}(x_j(k)) \tag{5}$$

$$\alpha_{ij}(x_j(k)) = e^{-\frac{\left(x_j(k)-c_{ij}\right)^2}{2s_{ij}^2}} \tag{6}$$

In Equation 3, the function $f_i[x(k)]$ is expressed as the first-order polynomial of input variables for the i^{th} fuzzy rule, and the output of each rule is expressed as follows:

$$f_i[\mathbf{x}(k)] = \sum_{j=1}^{m} \beta_{ij} x_j(k) + b_i \tag{7}$$

where β_{ij} is the weight of the i^{th} fuzzy rule and the j^{th} input variable, and b_i is the bias of the i^{th} fuzzy rule.

Therefore, in this case the FIS is referred to as a first-order Takagi-Sugeno-type FIS, because in the arbitrary i^{th} fuzzy rule output, f_i is a real value and is expressed as the first-order polynomial for the inputs.

Fig. 2 shows the calculation procedure of the FIS. The first layer indicates the input nodes that directly transmit the

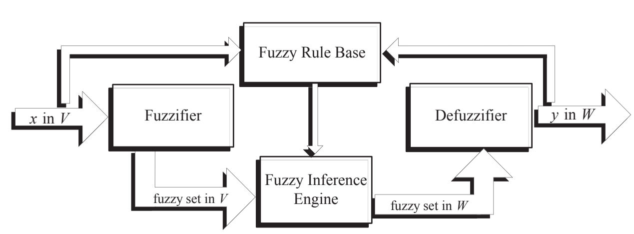

Fig. 1 – Fuzzy inference system (Mamdani-type).

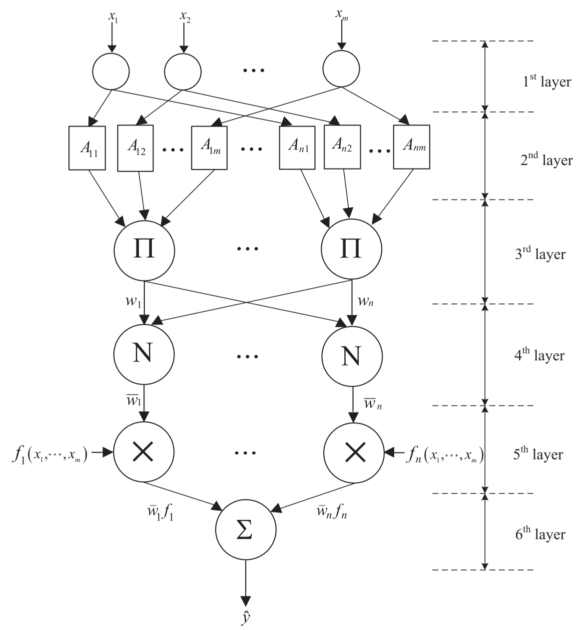

Fig. 2 – Fuzzy neural network.

input values to the next layer. Each output from the first layer is substituted into the membership function. The second layer indicates a fuzzification layer, which has the purpose of converting a crisp input value to a fuzzy value. The third layer indicates a product operator on the membership functions that is expressed as Equation 5. The fourth layer performs a normalization operation that is expressed as Equation 4. The fifth layer generates the output of each fuzzy *if/then* rule. Finally, the sixth layer conducts an aggregation of all the fuzzy *if/then* rules and is expressed as Equation 2.

Therefore, the output of the FIS by Equation 2 can be rewritten as:

$$\hat{y}(k) = \chi(k)^T \omega \tag{8}$$

Where

$$\omega = [\beta_{11} \cdots \beta_{n1} \cdots\cdots \beta_{1m} \cdots \beta_{nm}\ b_1 \cdots b_n]^T$$

and

$$\boldsymbol{\chi}(k) = [\overline{w}_1(k)x_1(k) \cdots \overline{w}_n(k)x_1(k) \cdots \overline{w}_1(k)x_m(k) \cdots \overline{w}_n(k)x_m(k) \times \overline{w}_1(k) \cdots x_n(k)]^T.$$

For a series of the N input/output data pairs, the following equation is derived from Equation 8:

$$\hat{\mathbf{y}} = \aleph\boldsymbol{\omega} \tag{9}$$

Where

$$\hat{y} = [\hat{y}(1)\hat{y}(2) \cdots \hat{y}(N)]^T$$

and

$$\aleph = [\chi(1)\chi(2) \cdots \chi(N)]^T.$$

The vector $\boldsymbol{\omega}$ is referred to as the consequent parameter vector and the matrix $\aleph$ consists of input data and membership function values. The output values of the FIS are expressed in a matrix $\aleph$ of $N \times (m+1)n$ dimensions and a parameter vector $\boldsymbol{\omega}$ of $(m+1)n$ dimensions.

2.2. *Training of the FIS*

The antecedent parameters related to the membership functions of Equation 6 were optimized using a genetic algorithm and the consequent parameters included in Equation 7 were optimized using a least square method. In genetic algorithms, the variables required to be optimized are encoded within the chromosome, and the superiority regarding each chromosome is judged by the fitness function.

In this study, the training data were used to optimize the parameters of the FNN model. The test data were used to verify the developed model and is different from the data set that was used for training. The fitness function in the following equation is intended to minimize the root mean square (RMS) error and maximum error:

$$F = \exp(-\mu_1 E_1 - \mu_2 E_2). \tag{10}$$

Where

$$E_1 = \sqrt{\frac{1}{N}\sum_{k=1}^{N_t}(y(k) - \hat{y}(k))^2},\ \ E_2 = \max_k(y(k) - \hat{y}(k)),\ \ N_t$$

is the number of training data values; E_1 is an RMS error, and E_2 is a maximum error. The variable $y(k)$ indicates the actual target value, whereas $\hat{y}(k)$ is the corresponding value that is predicted using the FNN model. If the antecedent parameters were fixed by the genetic algorithm, the matrix $\aleph$ was already known in the outputs of the proposed FNN model expressed by Equation 9. Therefore, the least squares method was used to determine the consequent parameter $\boldsymbol{\omega}$ of the fuzzy rules. The consequent parameter $\boldsymbol{\omega}$ was chosen to minimize the objective function, which consists of the square error between the target value $y(k)$ and its predicted value $\hat{y}(k)$, and it is expressed as follows:

$$J = \frac{1}{2}\sum_{k=1}^{N_t}(y(k) - \hat{y}(k))^2 = \frac{1}{2}\sum_{k=1}^{N_t}\left(y(k) - \boldsymbol{\chi}(k)^T\boldsymbol{\omega}\right)^2 = \frac{1}{2}(\mathbf{y}_t - \hat{\mathbf{y}}_t)^T(\mathbf{y}_t - \hat{\mathbf{y}}_t) \tag{11}$$

Where

$$y_t = [y(1)\ \ y(2)\ \cdots\ y(N_t)]^T$$

and

$$\hat{y}_t = [\hat{y}(1)\ \ \hat{y}(2)\ \cdots\ \hat{y}(N_t)]^T.$$

A solution for minimizing the above objective function can be obtained using the following equation:

$$\mathbf{y}_t = \aleph_t\boldsymbol{\omega} \tag{12}$$

Where

$$\aleph_t = [\chi(1)\chi(2) \cdots \chi(N_t)]^T.$$

The matrix $\aleph_t$ has $N_t \times (m+1)n$ dimensions and to solve the parameter vector $\boldsymbol{\omega}$, the inverse of the matrix $\aleph_t$ has to exist. By contrast, generally speaking, $\aleph_t$ does not have an inverse matrix, because usually the matrix $\aleph_t$ is not a square matrix.

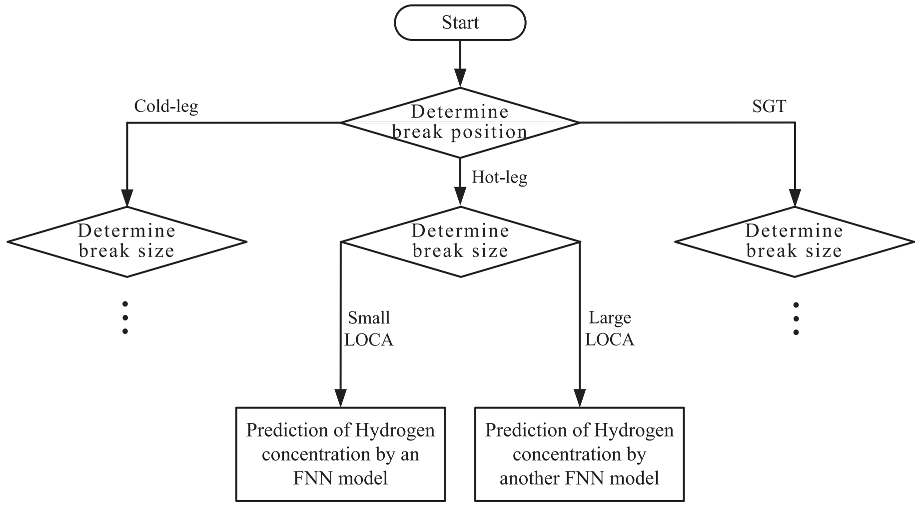

Fig. 3 – Prediction of hydrogen concentration using six integrated fuzzy neural network (FNN) models.

Therefore, the pseudo-inverse of the matrix $\aleph_t$ was used. The parameter vector $\boldsymbol{\omega}$ is solved easily using the pseudo-inverse matrix as shown below.

$$\boldsymbol{\omega} = \left(\aleph_t^T \aleph_t\right)^{-1} \aleph_t^T \mathbf{y}_t \qquad (13)$$

That is, the parameter vector $\boldsymbol{\omega}$ can be calculated from a series of input and output data pairs.

3. Data preparation

The proposed FNN model was subsequently applied to predicting the hydrogen concentration in the containment. Since hydrogen is accumulated in containment by leakage from the primary pressure boundary, a variety of LOCA simulations were conducted. It was assumed that safety systems including active safety injection systems did not actuate to model the LOCA that would be progressed into severe accidents to induce core damage and accelerate the hydrogen generation. The FNN model used two input signals, namely, the predicted value of the LOCA break size and the elapsed time after reactor shutdown. The training and test data for the proposed model were acquired by simulating severe accident scenarios using the MAAP4 code for OPR1000. The data used from simulation results are hydrogen concentration according to time.

In this study, the numerical simulations using the code were performed for a variety of break positions and break sizes of the LOCA. The LOCA break position was divided into hot-leg, cold-leg, and steam generator tube, and the break size steps were divided into 210 steps. The break sizes range from 1/10,000 of a double-ended guillotine break to half of a double-ended guillotine break for hot-leg and cold-leg LOCAs, and the break sizes range from 1 to 210 tube ruptures for SGTR accidents.

Incidents involving LOCAs require the LOCA position and break size to be identified and predicted, because these values are not detected. Therefore, the LOCA break size signal, which is an input signal for the FNN model, was obtained from previous studies in which algorithms were developed for the purpose of determining this signal [18–20]. These studies also established that it was possible to predict the LOCA break size accurately with an RMS error of about 0.4% [19]. For this reason, the LOCA break size can be used as an input variable for predicting the hydrogen concentration in containment.

The simulations resulted in 630 cases of severe accident scenarios. The data consisted of 210 pieces for each of the hot-leg LOCA, cold-leg LOCA, and SGTR.

4. Application to predicting the hydrogen concentration

In the event of a severe accident, it would be necessary to examine whether the hydrogen concentration in the containment is excessive. The input variables for the

Table 1 – Performance of the fuzzy neural network model [hot-leg loss of coolant accident (LOCA)].

Number of fuzzy rules	Small LOCA				Large LOCA				All break sizes	
	Training data		Test data		Training data		Test data		Test data	
	RMS error (%)	Max. error (%)	RMS error (%)	Max. error (%)	RMS error (%)	Max. error (%)	RMS error (%)	Max. error (%)	RMS error (%)	Max. error (%)
5	16.92	118.00	20.81	108.19	0.86	17.08	1.18	6.18	11.14	108.19
10	8.70	65.04	8.10	36.83	0.86	17.82	1.21	7.20	2.68	21.89
30	6.97	69.87	5.18	21.85	0.66	16.19	0.94	6.67	**1.83**	**13.29**
50	5.80	62.61	5.87	33.11	0.60	14.92	0.82	6.37	3.65	33.11

RMS, root mean square.
Values in bold font are data of the most optimized values.

Table 2 – Performance of the fuzzy neural network model [cold-leg loss of coolant accident (LOCA)].

Number of fuzzy rules	Small LOCA				Large LOCA				All break sizes	
	Training data		Test data		Training data		Test data		Test data	
	RMS Error (%)	Max. Error (%)	RMS Error (%)	Max. Error (%)	RMS Error (%)	Max. Error (%)	RMS Error (%)	Max. Error (%)	RMS Error (%)	Max. Error (%)
5	8.51	72.30	12.13	45.36	2.62	28.89	3.42	12.90	7.35	43.31
10	6.29	68.11	9.43	43.24	2.34	20.47	3.00	7.87	5.57	43.24
30	5.19	63.24	7.81	39.30	2.04	19.07	2.73	9.97	**4.98**	**37.59**
50	4.56	67.32	8.09	55.07	1.96	18.58	2.71	9.46	6.36	55.07

RMS, root mean square.

Table 3 – Performance of the fuzzy neural network model (steam generator tube rupture).

Number of fuzzy rules	Small LOCA				Large LOCA				All break sizes	
	Training data		Test data		Training data		Test data		Test data	
	RMS error (%)	Max. error (%)	RMS error (%)	Max. error (%)	RMS error (%)	Max. error (%)	RMS error (%)	Max. error (%)	RMS error (%)	Max. error (%)
5	11.92	70.39	16.62	41.85	14.25	74.58	19.84	61.79	18.66	61.79
10	11.92	62.50	15.83	40.32	13.57	72.42	20.79	67.72	18.19	52.35
30	11.03	70.12	14.27	43.10	11.07	97.44	15.75	46.09	14.93	46.09
50	10.12	77.83	12.58	30.94	10.58	110.27	14.57	50.00	**13.41**	**45.28**

LOCA, loss of coolant accident; RMS, root mean square.

prediction of the hydrogen concentration are the elapsed time after reactor shutdown and the predicted LOCA break size. Therefore, FNN models were developed to assess both large and small break LOCAs as well as the break position. The FNN models were optimized by both the genetic algorithm and the least-squares method.

Fig. 3 shows the six integrated FNN models (each consisting of 3 break positions, each of which has been subdivided into 2 break size groups) that were developed in this study to predict the hydrogen concentration. Furthermore, three different types of FNN models were developed according to the LOCA position, namely, hot-leg, cold-leg, and SGTR. In addition, two different types of FNN models were developed depending on whether the LOCA break size is small or large. In the case of hot-leg and cold-leg LOCAs, the break sizes in each of these were further divided into two groups, with the 30 smaller break sizes forming one group and the remaining 180 larger break sizes forming the other group. Similarly, in the case of

Table 4 – Performance of fuzzy neural network model assuming loss of coolant accident (LOCA) break size prediction error (random prediction error < 5%).

Number of fuzzy rules	Hot-leg LOCA		Cold-leg LOCA		SGTR	
	Training data		Training data		Test data	
	RMS error (%)	Max. error (%)	RMS error (%)	Max. error (%)	RMS error (%)	Max. error (%)
5	11.70	113.88	7.36	43.21	19.01	61.06
10	2.62	20.89	5.48	41.90	**18.75**	**51.20**
30	**1.78**	**12.76**	**4.96**	**36.23**	17.45	71.88
50	3.93	35.99	6.33	54.21	15.50	56.67

RMS, root mean square; SGTR, steam generator tube rupture.

Table 5 – Performance of fuzzy neural network model assuming loss of coolant accident (LOCA) break size prediction error (5% over-prediction).

Number of fuzzy rules	Hot-leg LOCA		Cold-leg LOCA		SGTR	
	Training data		Training data		Test data	
	RMS error (%)	Max. error (%)	RMS error (%)	Max. error (%)	RMS error (%)	Max. error (%)
5	10.16	98.14	7.56	43.48	**19.49**	**58.79**
10	2.88	23.13	5.87	44.79	23.20	96.53
30	**2.53**	**14.00**	**5.26**	**39.24**	24.71	99.15
50	6.97	53.72	6.46	56.04	435.05	4.34×10^3

RMS, root mean square; SGTR, steam generator tube rupture.

SGTR, the break sizes were also divided into two groups: the 100 smaller break sizes were grouped together while the remaining 110 larger break sizes formed the second group. The reason that two groups were used was that this grouping provided better results than that of using only one group.

The test data were different from the data used to develop the FNN model, and consisted of the elapsed time after reactor shutdown, the predicted LOCA break size, and the hydrogen concentration. For this study, 100 data points in each of the LOCA break positions, namely, hot-leg and cold-leg LOCA, and SGTR, were selected as test data points.

The parameter values that are concerned with the genetic algorithm and the FIS are as follows: the crossover probability is 100%, the mutation probability is 5%, and the population size is 20.

Tables 1–3 show the performance results that were obtained with the developed FNN model for the three break positions of

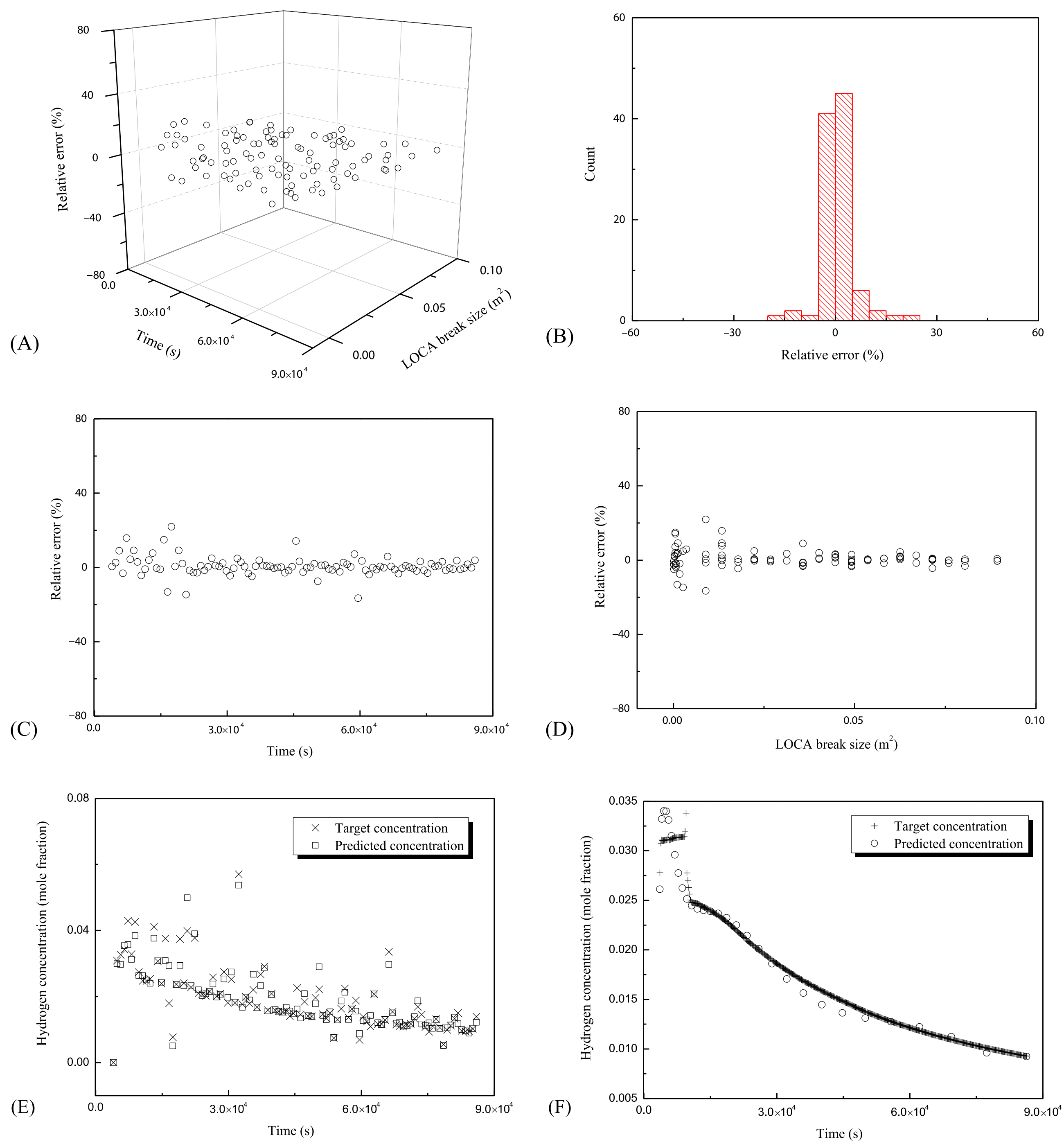

Fig. 4 – Prediction performance of fuzzy neural network model in hot-leg small loss of coolant accident (LOCA). (A) Relative prediction error of hydrogen concentration versus elapsed time and loss of coolant accident break size. (B) Relative prediction error histogram of hydrogen concentration. (C) Relative prediction error of hydrogen concentration versus elapsed time. (D) Relative prediction error of hydrogen concentration versus LOCA break size. (E) Hydrogen concentration versus time. (F) Hydrogen concentration versus time at a specific LOCA break size.

hot-leg, cold-leg, and SGTR, respectively. For the test data of the hot-leg LOCA, the RMS errors were approximately 11.14%, 2.68%, 1.83%, and 3.65% for the FNN model with five, 10, 30, and 50 fuzzy rules, respectively. For the test data of the cold-leg LOCA, the RMS errors were approximately 7.35%, 5.57%, 4.98%, and 6.36% for the FNN model with five, 10, 30, and 50 fuzzy rules, respectively. Further, for the test data of the SGTR, the RMS errors were approximately 18.66%, 18.19%, 14.93%, and 13.41% for the FNN model with five, 10, 30, and 50 fuzzy rules, respectively. Therefore, the FNN model with 30 fuzzy rules proved to be the most accurate for predicting the hydrogen concentration in both hot-leg and cold-leg LOCA, while the FNN model with 50 fuzzy rules was shown to be the most accurate for predicting the hydrogen concentration in SGTR.

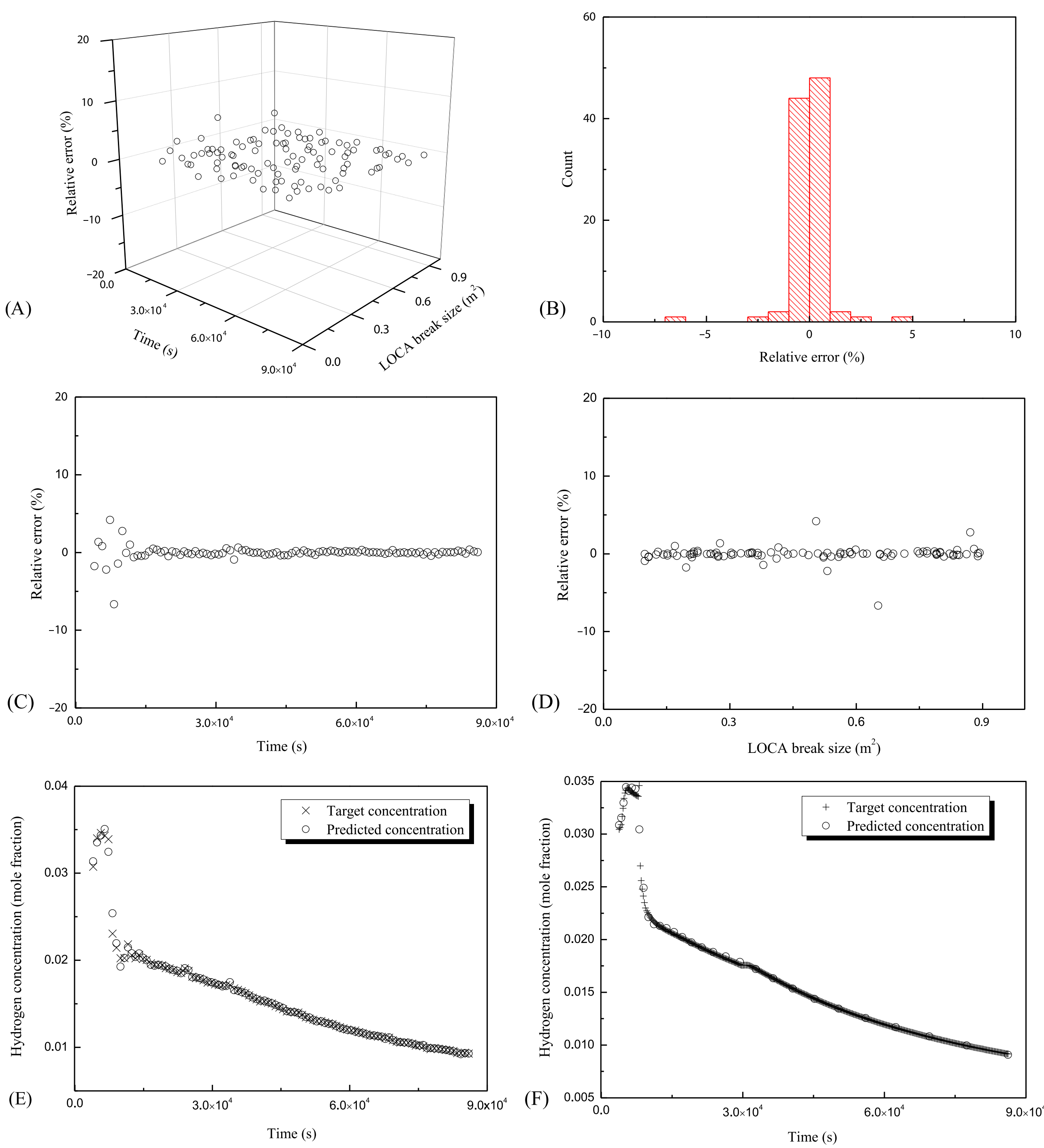

Fig. 5 – Prediction performance of fuzzy neural network model in hot-leg large loss of coolant accident (LOCA). (A) Relative prediction error of hydrogen concentration versus elapsed time and loss of coolant accident break size. (B) Relative prediction error histogram of hydrogen concentration. (C) Relative prediction error of hydrogen concentration versus elapsed time. (D) Relative prediction error of hydrogen concentration versus LOCA break size. (E) Hydrogen concentration versus time. (F) Hydrogen concentration versus time at a specific LOCA break size.

Table 6 – Performance of the optimized fuzzy neural network models.

Break position	No LOCA break size prediction error		Random LOCA break size prediction error under 5%		5% LOCA break size over-prediction error	
	RMS error (%)	Max. error (%)	RMS error (%)	Max. error (%)	RMS error (%)	Max. error (%)
Hot-leg LOCA	1.83	13.29	1.78	12.76	2.53	14.00
Cold-leg LOCA	4.98	37.59	4.96	36.23	5.26	39.24
SGTR	18.66	61.79	19.01	61.06	19.49	58.79

LOCA, loss of coolant accident; RMS, root mean square; SGTR, steam generator tube rupture.

Previously, the LOCA break size could be predicted accurately within 60 seconds after reactor shutdown with an RMS error of about 0.4% [19]. However, it is necessary to investigate the effect of error propagation, which is caused by errors in the input signals, even if they are small. Table 4 shows the performance of the FNN models in the case in which the LOCA break size was assumed to be predicted with a random error of < 5%. In this case, the performance degradation of the FNN models resulting from the existence of input errors is not visible. Table 5 shows the performance of the FNN models in the case in which the LOCA break size was assumed to have a 5% over-prediction error. In the case of SGTR, the FNN model with 50 fuzzy rules was determined to have an over-fitting characteristic, whereas the FNN model with five fuzzy rules was found to perform the best.

Figs. 4 and 5 show the hydrogen concentration predicted by the optimized FNN models, together with their prediction errors, for the test data of the hot-leg small and hot-leg large LOCAs, respectively. Figs. 4A and 5A show the prediction errors of the hydrogen concentration versus the elapsed time and the LOCA break size for the hot-leg small and large LOCAs, respectively. Fig. 4B, 5B show the prediction error histogram that was used to verify the error distribution of the hydrogen concentration. Figs. 4C and 5C show the prediction errors of the hydrogen concentration versus the elapsed time. Figs. 4D and 5D show the prediction errors of the hydrogen concentration versus the break size. Figs. 4E and 5E show the hydrogen concentration versus the elapsed time. The hydrogen concentration data are scattered due to the different LOCA break sizes involved. Figs. 4F and 5F show the hydrogen concentration versus the elapsed time at a specific LOCA break size. The corresponding plots relating to cold-leg LOCA and SGTR showed similar trends and were omitted from this paper to save space.

Table 6 shows the performance of the optimized FNN models, i.e., those with 30 fuzzy rules for the hot-leg and cold-leg LOCAs, and five fuzzy rules for the SGTRs. This table shows that the RMS errors for the test data were approximately 1.83%, 4.98%, and 18.66% for the hot-leg and cold-leg LOCAs, and the SGTR, respectively. In cases in which the break size of the LOCAs was assumed to be predicted with a random error of < 5%, the RMS errors for the test data were approximately 1.78%, 4.96%, and 19.01% for the hot-leg and cold-leg LOCAs, and the SGTR, respectively. Moreover, in cases in which the LOCA break size is assumed to have a 5% over-prediction error, the RMS errors for the test data were approximately 2.53%, 5.26%, and 19.49% for the hot-leg and cold-leg LOCAs, and the SGTR, respectively. Therefore, the FNN models have been shown to be capable of accurately predicting the hydrogen concentration under severe accident circumstances.

5. Conclusion

Within reactor containment, it is necessary to prevent the local hydrogen concentration from exceeding 4% to prevent the hydrogen from exploding. This paper proposes an FNN model, which was developed to predict the hydrogen concentration in containment under severe accident circumstances. As its input, the model uses variables for the time that has elapsed after reactor shutdown and the predicted LOCA break size. The FNN model was developed and verified using the simulation data of the MAAP4 code for OPR1000. The developed FNN model is able to predict the hydrogen concentration in containment at a specific time using the predicted LOCA break size and the changing trend in the hydrogen concentration in containment after a LOCA.

The RMS errors of the FNN model were approximately 1.83%, 4.98%, and 18.66% for the hot-leg and cold-leg LOCAs, and the SGTR, respectively. The prediction results show the FNN model is capable of accurately predicting the hydrogen concentration for hot-leg and cold-leg LOCAs. The developed FNN model is expected to be helpful for providing effective information for operators in severe accident situations.

Conflicts of interest

The author declares no conflicts of interest.

Acknowledgments

This work was supported by a Nuclear Research & Development Program of the National Research Foundation of Korea (NRF) grant funded by the Korean government (MSIP), (Grant No. 2012M2B2B1055611).

REFERENCES

[1] J.W. Hines, D.J. Wrest, R.E. Uhrig, Signal validation using an adaptive neural fuzzy inference system, Nucl. Technol. 119 (1997) 181–193.

[2] M.G. Na, A neuro-fuzzy inference system for sensor failure detection using wavelet denoising, PCA and SPRT, Journal of the Korean Nucl. Soc. 33 (2001) 483–497.

[3] J. Garvey, D. Garvey, R. Seibert, J.W. Hines, Validation of on-line monitoring techniques to nuclear plant data, Nucl. Eng. Technol. 39 (2007) 149–158.
[4] E.B. Bartlett, R.E. Uhrig, Nuclear power plant diagnostics using an artificial neural network, Nucl. Technol. 97 (1992) 272–281.
[5] M. Marseguerra, E. Zio, Fault diagnosis via neural networks: The Boltzmann machine, Nucl. Sci. Technol. 117 (1994) 194–200.
[6] Y.G. No, J.H. Kim, M.G. Na, D.H. Lim, K.I. Ahn, Monitoring severe accidents using AI techniques, Nucl. Eng. Technol. 44 (2012) 393–404.
[7] A. Gofuku, H. Yoshikawa, S. Hayashi, K. Shimizu, J. Wakabayashi, Diagnostic techniques of a small-break loss-of-coolant accident at a pressurized water reactor plant, Nucl. Technol. 81 (1988) 313–332.
[8] M.G. Na, S.M. Lee, S.H. Shin, D.W. Jung, S.P. Kim, J.H. Jeong, B.C. Lee, Prediction of major transient scenarios for severe accidents of nuclear power plants, IEEE Trans. Nucl. Sci. 51 (2004) 313–321.
[9] S.W. Cheon, S.H. Chang, Application of neural networks to a connectionist expert system for transient identification in nuclear power plants, Nucl. Technol. 102 (1993) 177–191.
[10] Y. Bartal, J. Lin, R.E. Uhrig, Nuclear power plant transient diagnostics using artificial neural networks that allow don't-know classifications, Nucl. Technol. 110 (1995) 436–449.
[11] S.H. Park, J.H. Kim, K.H. Yoo, M.G. Na, Smart sensing of the RPV water level in NPP severe accidents using a GMDH algorithm, IEEE Trans. Nucl. Sci. 61 (2014) 931–938.
[12] S.H. Park, D.S. Kim, J.H. Kim, M.G. Na, Prediction of the reactor vessel water level using fuzzy neural networks in severe accident circumstances of NPPs, Nucl. Eng. Technol. 46 (2014) 373–380.
[13] M.G. Na, H.Y. Yang, D.H. Lim, A soft-sensing model for feedwater flow rate using fuzzy support vector regression, Nucl. Eng. Technol. 40 (2008) 69–76.
[14] J.S. Roger Jang, C.T. Sun, Functional equivalence between radial basis function networks and fuzzy inference systems, IEEE Trans. Neural Networks 4 (1993) 156–159.
[15] MAAP4 - Modular Accident Analysis Program for LWR Power Plants User's Manual, prepared by Fauske & Associates, LLC for EPRI, Project RP3131-02, May 1994 – June 2005
[16] T. Takagi, M. Sugeno, Fuzzy identification of systems and its applications to modeling and control, IEEE Trans. Syst. Man. Cybern. SMC-15 (1985) 116–132.
[17] E.H. Mamdani, S. Assilian, An experiment in linguistic synthesis with a fuzzy logic controller, Int. J. Man Mach. Stud. 7 (1975) 1–13.
[18] S.H. Lee, Y.G. No, M.G. Na, K.I. Ahn, S.Y. Park, Diagnostics of loss of coolant accidents using SVC and GMDH models, IEEE Trans. Nucl. Sci. 58 (2011) 267–276.
[19] M.G. Na, W.S. Park, D.H. Lim, Detection and diagnostics of loss of coolant accidents using support vector machines, IEEE Trans. Nucl. Sci. 55 (2008) 628–636.
[20] M.G. Na, S.H. Shin, D.W. Jung, S.P. Kim, J.H. Jeong, B.C. Lee, Estimation of break location and size for loss of coolant accidents using neural networks, Nucl. Eng. Design 232 (2004) 289–300.